UCRL-101870
PREPRINT

PROPAGATION OF FLUID-DRIVEN FRACTURES IN JOINTED ROCK.

PART 1: DEVELOPMENT AND VALIDATION OF METHODS OF ANALYSIS

F. E. Heuze*
R. J. Shaffer*
A. R. Ingraffea**
R. H. Nilson***

*Lawrence Livermore National Laboratory, Livermore, CA
**Cornell University, Ithaca, NY
***S-Cubed, La Jolla, CA.

This paper was submitted for publication in the
International Journal of Rock Mechanics and Mining Science.

September, 1989

Lawrence Livermore National Laboratory

This is a preprint of a paper intended for publication in a journal or proceedings. Since changes may be made before publication, this preprint is made available with the understanding that it will not be cited or reproduced without the permission of the author.

INDEX

		Page
	ABSTRACT	ii
I.	INTRODUCTION	1
2.	THE STEADY-STATE ANALYSIS	1
	2.1 Elements of the Steady-State Model	2
	2.2 Analytical Verification	2
	2.3 Validation Against Physical Models	3
	2.4 Examples of Steady-State Analyses	4
	2.4.1 Crack curvature near a lens	4
	2.4.2 Hydrofracturing in coal	6
	2.4.3 Fracture and flow in a jointed rock mass	9
3.	THE TIME-DEPENDENT MODEL	12
	3.1 Rationale for the New Developments	12
	3.2. The FAST Fluid Dynamics Model	12
	3.2.1 Governing equations	12
	3.2.2 Numerical solution procedure	14
	3.3 The Coupling of FAST to FEFFLAP	15
	3.4 Verification/Validation of FEFFLAP 2.0/FAST	16
	3.4.1 Analytical solution for gas-driven fractures with constant borehole pressure	16
	3.4.2 Analytical solution for laminar incompressible fluid flow, with constant flow rate	17
	3.4.3 Validation against physical block tests	18
	3.5 Examples of Applications	23
4.	SUMMARY - DISCUSSION	26
5.	REFERENCES	27
6.	ACKNOWLEDGMENTS	30

ABSTRACT

We have developed a new method of analysis to describe the propagation of induced fluid-driven fractures in rock masses which contain pre-existing discontinuities such as joints, faults, bed interfaces, lens boundaries, etc. The analysis is based on a 2-dimensional model, with coupled solid mechanics, fracture mechanics, and fluid mechanics. The solid and fracture mechanics are solved by an implicit finite element approach which provides for mixed-mode (I and II) fracture propagation in arbitrary stress fields. The fluid mechanics capability first was established for steady-state conditions, using a finite element formulation for flow between parallel surfaces. This initial coupling resulted in the version 1.0 of the FEFFLAP model (Finite Element Fracture and Flow Analysis Program). This version was verified against analytical solutions, and tested for validation against results of hydrofracturing in blocks of rock simulants containing an interface, under biaxial loading, as described in Part 2, the companion paper to this publication.

The developments were then extended to the time-dependent domain by replacing the original fluid flow analysis with an analysis based on the FAST fluid dynamics module. The pressure profile inside the crack and the crack velocity are provided by a one-dimensional analytical formulation, corresponding to a constant-height fracture. Both arbitrary flow-rate and borehole pressure conditions can be simulated; these may correspond respectively to conventional two-wing hydrofracturing, and gas-driven tailored-pulse loading for multiple fractures. The model has been verified against analytical time-dependent solutions for fracturing in permeable and impermeable media. The new coupled model also has been validated against controlled physical tests involving hydrofracturing of blocks containing sandstone lenses, with the blocks loaded independently in three orthogonal directions. These tests are also described in the companion paper.

These new analysis tools can be used for a wide variety of applications such as obtaining a better understanding of the stimulation of unconventional gas reservoirs, i.e., lenticular sandstones, coal beds, and Devonian shales, or making improvements in the design of underground waste disposal by hydrofracturing, or enhancing the fracturing of geothermal reservoirs.

1. INTRODUCTION

The fracturing of rocks underground, with pressurized fluids, is a common procedure for attempting to enhance the productivity of certain gas and oil reservoirs [1-6] and to estimate in-situ stresses in rock masses [7]; it also has been used to dispose of unwanted liquid wastes, underground [8]. To assist in designing such fracturing injections, a significant number of mathematical simulations have been developed; excellent overviews of these models have been published [1-5].

The remarkable common thread to all these models is that they assume the rock medium to be continuous. This is noticeable indeed since it is well known that rock masses in place are very seldom, even approximately, continuous; typically they are transected by various types of discontinuities such as joints, shear zones, faults, bedding contacts, lens boundaries, etc. More importantly, it is also known that these interfaces can have a strong detrimental effect on the ability to control and extend fluid-driven fractures. Recent, innovative field tests involving a "mine-back" of fracture paths have provided vivid documentation of fractures stopping at interfaces, or branching out sideways, or reinitiating in a stepped fashion after stopping at a contact [9].

With the above considerations in mind, we have pursued a course of development and validation of new analysis methods to describe the propagation of fluid-driven fractures in discontinuous media [10-11]. These are embodied in FEFFLAP (Finite Element Fracture and Flow Analysis Program), a two-dimensional implicit numerical model which has capabilities to simulate both steady-state flow in fractures and joints, and time-dependent fluid-driven fracturing. These two aspects are taken up separately, next.

2. THE STEADY-STATE ANALYSIS

The steady-state model, FEFFLAP Version 1.0, was constructed of several building blocks, to achieve a capability for coupled solid mechanics, fracture mechanics, and flow analysis.

2.1 Elements of the Steady-State Model

The components assembled into a new model were (1) the FEFAP two-dimensional implicit finite element program for solid and fracture mechanics [12], which modeled only continuous media, (2) the joint finite elements with sophisticated constitutive laws as developed in the JPLAXD code [13], which were incorporated in FEFAP, and (3) the flow-in-fracture algorithms contained in the JTFLOW finite element model [14]. The fracture mechanics algorithms, the joint models, the flow equations, and the logic to couple the analysis were reported in detail, previously [15,16]. This information will not be repeated, for the sake of brevity, and more particularly because this work was only considered to be a prelude to the development of the time-dependent analysis. For completeness, however, we will present summaries of verification and validation studies for FEFFLAP 1.0, as well as examples of applications.

2.2 Analytical Verification

FEFFLAP 1.0 was tested on a cracked borehole problem (standard hydrofrac geometry) by calculating Mode I stress intensity factors for two types of loading: a remote biaxial tensile stress, and uniformly pressurized borehole and cracks. The results were compared to established values [17] to obtain an estimate of the model's accuracy. For both types of loading, each crack length was 1.5 times the borehole radius. The Mode I stress intensity factor calculated in FEFFLAP was 7 percent higher than the established value for both cases. These results are quite good when one considers the coarse finite element mesh that was used. In addition, the mesh was truncated at 10 times the borehole radius while the established values correspond to an infinite medium.

The multicrack capability of FEFFLAP was verified against an analytical solution for six pressurized cracks emanating from a borehole [18]. The geometry of the cracks in half plane symmetry is shown in Figure 1; it has 6-fold symmetry. The borehole and the cracks are subject to a constant pressure P. Table 1 lists the values for the nondimensional Mode I stress intensity factors for each crack tip. The quantity μ is the ratio of crack length plus borehole radius, to borehole radius. There is a slight variation in the values of μ for the three cracks. This is due to the fact that the crack tip locations are identified by positioning a cursor on the computer screen.

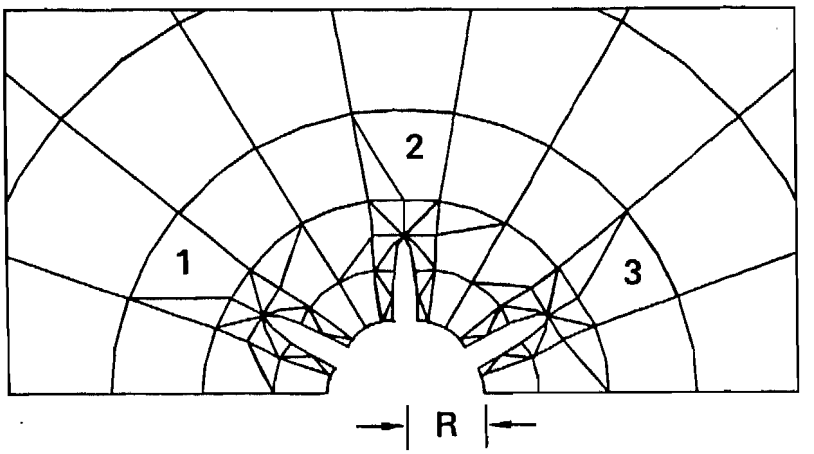

Figure 1. FEFFLAP 1.0 Analysis of Multiple Crack Propagation, for Comparison with Analytical Results.

Every crack tip should have the same value of stress intensity. Table 1 shows that the FEFFLAP values vary by no more than 4% from the analytical ones.

Table 1. Comparison of FEFFLAP 1.0 Results with Analytically-Obtained Results [18] for Multiple Cracks.

Crack Number	μ	$K_I/P\sqrt{\pi\mu R}$
1	2.679	0.779
2	2.678	0.781
3	2.676	0.775
Reference [18]	$\rangle$ 1.5	0.743

2.3 Validation Against Physical Models

The steady-state numerical model was used to simulate results from 2 tests of a 13-test series of hydrofracturing tests in hydrostone blocks loaded biaxially. Details of these tests are given in the companion paper, on physical modeling, and in references [19, 20].

The basic geometry is shown in Figure 2. The problem involved two types of hydrostone separated by an interface, and also included the steel platens that were used to load the blocks. Thus three different solid material types were used in the analysis. Four joint-interface types were required: (1) the interface between the two hydrostone materials, (2) the interfaces between steel platens and the hydrostone, (3) the joint elements that are inserted into the crack as it propagates,

and (4) a set of joint elements around the interior of the borehole, which provides a convenient way to pressurize the hole. The last two joint types were necessary for the fluid flow part of the analysis.

In order to determine the adequacy of FEFFLAP, a 2-D code, to handle the 3-D geometry of the blocks, the stresses in the mid-vertical section of the block were calculated both with a plane stress FEFFLAP solution, and with JROC3D, a 3-D jointed block code developed at Imperial College, in London [21] and enhanced by F. Heuze at LLNL. Results agreed to better than 1% [20].

Then, two of the tests were analyzed with FEFFLAP using the mesh shown in Figure 3. Figure 4 shows the results of a FEFFLAP analysis of one experiment in which the crack reinitiated from the interface; for this case the vertical and horizontal stresses were 12.4 and 5.2 MPa respectively, and the peak borehole pressure was 23.4 MPa. The borehole pressure required in FEFFLAP to reinitiate the crack was higher than that in the experiment, and the reinitiated crack was offset. It is possible that the cracks crossed the interface dynamically in the experiments because they went straight through the interface. In Figure 5, the FEFFLAP analysis replicated another experiment in which a crack stopped at the interface; vertical and horizontal loading stresses were 4.8 and 0.7 MPa, respectively, and the peak pressure in the borehole was 19.3 MPa.

2.4 Example of Steady-State Analyses

2.4.1 Crack curvature near a lens

Figure 6 shows the analysis of a hydrofracture initiated parallel to a layer boundary to determine under what conditions the crack would turn toward or away from the interface. When the layer is twice as stiff as the surrounding medium, the crack tends to curve toward the layer (points A and B on Fig. 6). When the surrounding medium is twice as stiff as the layer, the crack tends to curve away from the layer (points C and D). The amount of curvature also depends on the relative values of the in-situ stresses parallel and perpendicular to the layer boundary. When the stresses approach the hydrostatic state, the fractures tend to curve less than when the maximum stress is aligned with the initial crack direction. ($\sigma_x = 2.25\ \sigma_y$ for points A and D, and $\sigma_x = \sigma_y$ for points B and C). These results can help provide some insight in the stimulation mechanics of lenticular gas reservoirs.

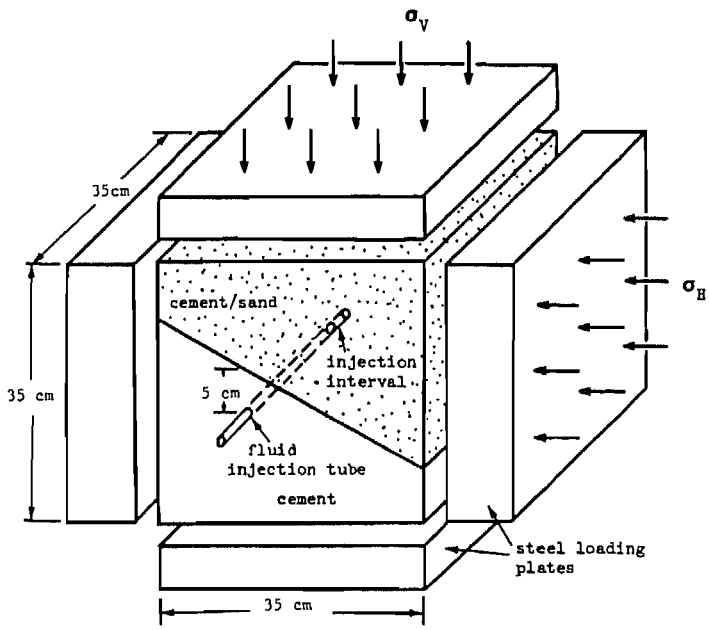

Figure 2. Geometry of Hydrofracturing in Jointed Blocks Made of Two Different Materials.

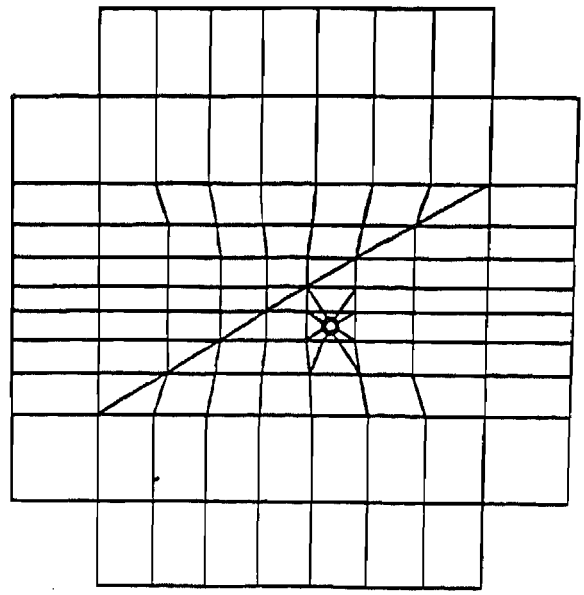

Figure 3. Finite Element Mesh for the Jointed Block Hydrofrac Analysis with FEFFLAP.1.0.

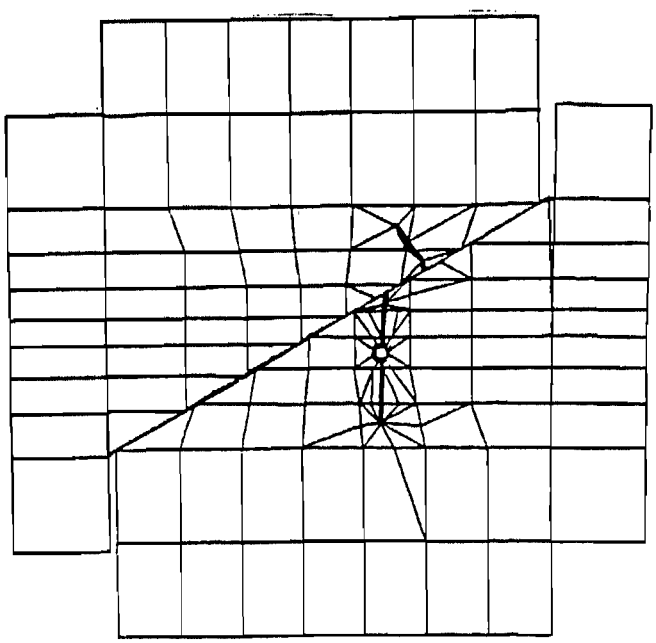

Figure 4. Fracture Crosses Interface, and Restarts Offset (σ_v = 12.4 MPa, σ_h = 5.2 MPa).

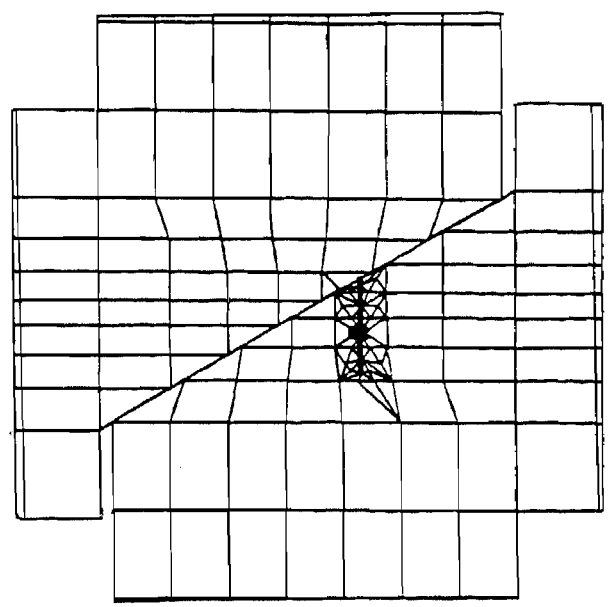

Figure 5. Fracture Does Not Cross the Interface (σ_v = 4.8 MPa, σ_h = 0.7 MPa).

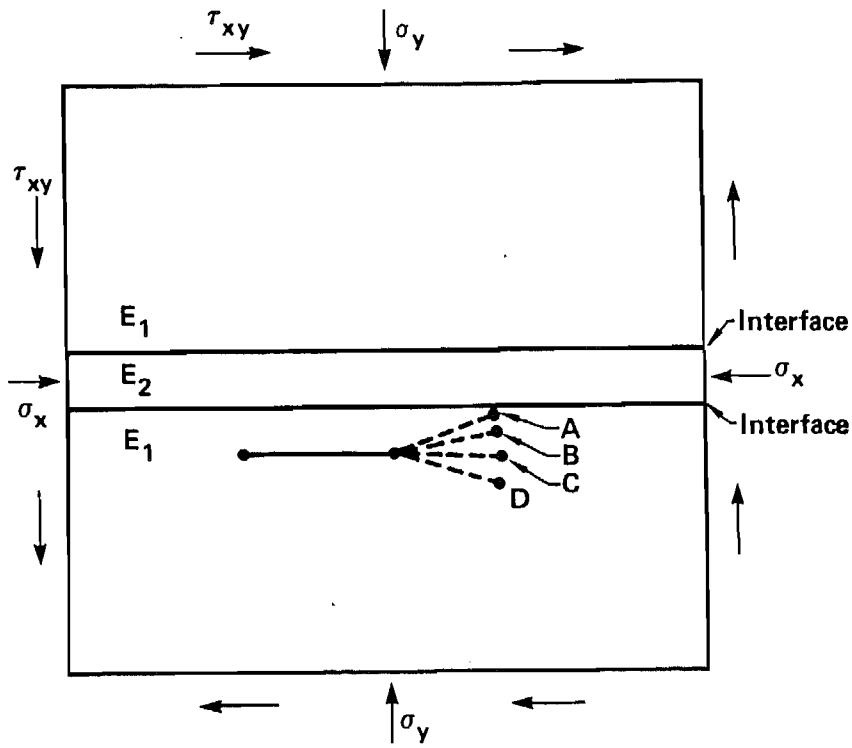

	E_2/E_1	σ_x/σ_y
A	2.0	2.25
B	2.0	1.00
C	0.5	1.00
D	0.5	2.25

Figure 6. Behavior of a Hydrofracture Near a Rock Layer Interface.

2.4.2 Hydrofracturing in coal

Figure 7 shows a plan view of a hydrofracture in the Oak Grove Mine near Birmingham, Alabama. An analysis was done with FEFFLAP 1.0 to determine why the fracture went into the roof rock. The results indicate that no net tension would be created in the shale roof rock due to the coal hydrofracture. However, it was surmised that inflation of an existing flaw in the shale roof could occur if fluid got to it, and this new crack then could propagate into the roof.

The geometry of Figure 8 was constructed to model the Blue Creek coal seam. It also includes the one-foot thick Marylee seam for completeness. There are five horizontal joint systems; all of them are coal-shale interfaces except for the coal-coal interface at the bottom of the hydrofrac. This geometry represents a cross section of about 12m x 12 m. The hydrofracture in the coal is inflated. An analysis was done to obtain the stresses and determine if there were any nonlinear behavior of the slickensided joints near the hydrofracture. There was no joint inelastic slip.

Figure 9 represents a "blow-up" of the hydrofracture - shale intersection. This grid corresponds to an area 60 cm wide by 52 cm high. This analysis was done for the

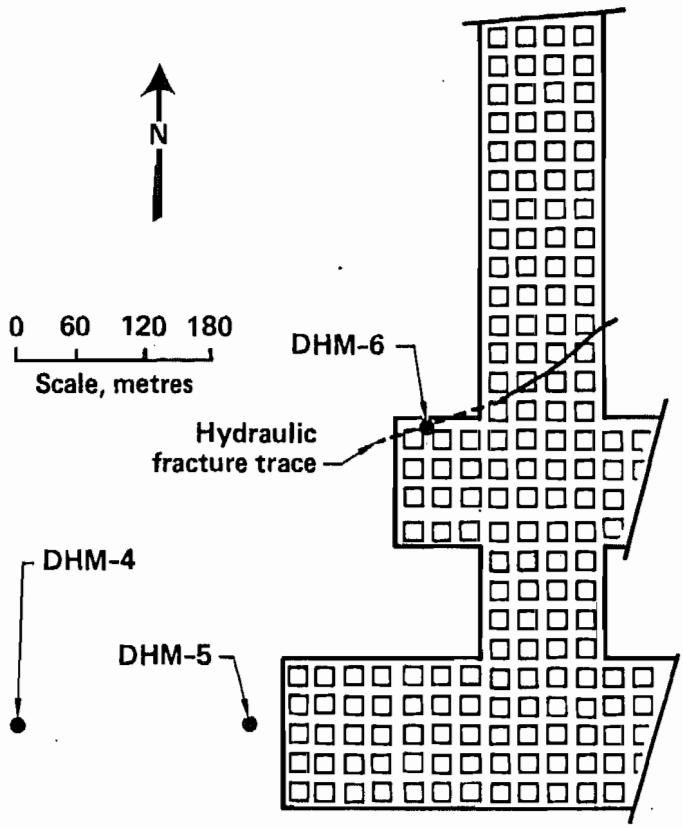

Figure 7. Hydrofracturing at the Oak Grove Mine, near Birmingham, Alabama, in the Blue Creek Coal Seam.

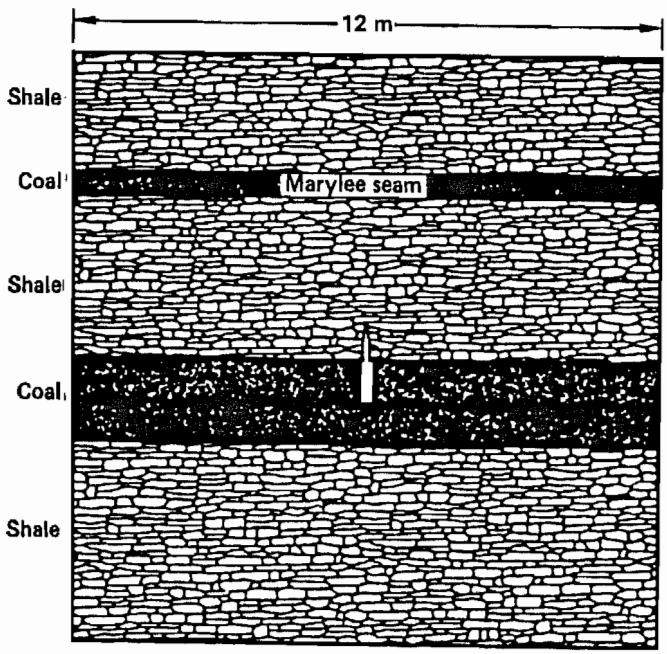

Figure 8. Model of the Hydrofracture in Coal, Extending into the Shale Roof.

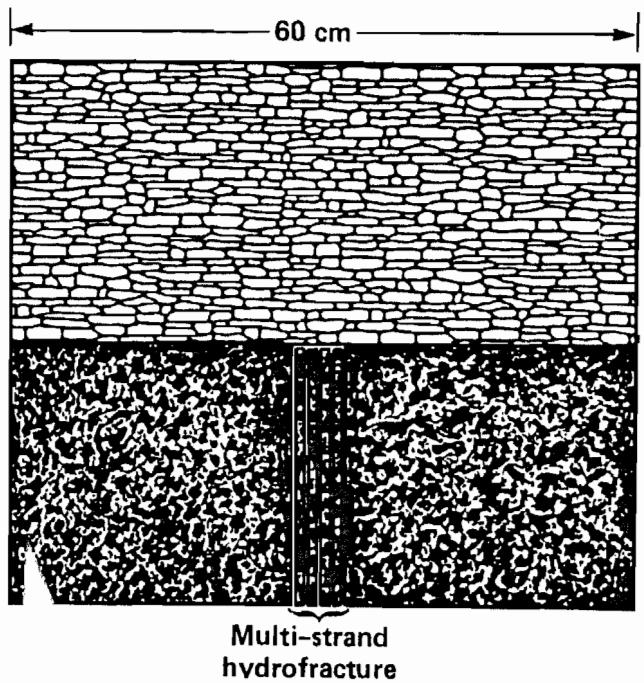

Fi 9. Detailed Geometry for FEFFLAP Analysis of the Fracture at the Interface.

same reasons as above, except that here the details are fine enough to look at five face cleats and treat the fracture as being 5 cm wide. The boundary conditions for this analysis were obtained from the previous analysis; i.e., the stresses corresponding to the perimeter of Figure 9 were extracted from the results of stress analysis on the larger grid. As before, there was no joint inelastic slip at these loads. Note that if this slip occurred, it would deconcentrate stresses and, for our particular problem, it would tend to retard or diminish the creation of tensile stress across the interface in the shale. The stresses just across the interface did not show tension above the 5 cm crack. Indeed, there was compression, with the horizontal component in the 2.1 to 3.5 MPa range. What happened, then? We know from field observations that the shale had a dilated proppant-filled crack.

A possible explanation was proposed as follows: suppose that there is a flaw of some height h in the shale, that intersects the coal-shale interface. Suppose further that the 5 cm wide hydrofracture comes in contact with this flaw. If fluid can get into this crack, even though it is under compression the crack could extend. There is a way for this to occur - namely - a mismatch of the flaw's surfaces. Assuming fluid penetration due to mismatch, the problem to solve with FEFFLAP is the minimum height h of the pre-existing crack to allow the fluid to extend it. Five calculations were run: crack lengths of 1/2 cm and 2 cm with the mesh of Figure 9, and crack lengths of 7, 12, and 62 cm with the mesh of Figure 8. Figure 8, for example, shows the 62 cm crack in the shale overburden. Table 2 summarizes the results of the calculations in terms of stability. It shows the Mode I stress intensity factor K_I and the load factor, F, for each calculation. A load factor $F < 1$ means crack instability. If the load factor is greater than 1, the crack will become unstable when the load vector is multiplied by F. The shale fracture toughness was taken as $K_{IC} = 1.2$ MPa$\sqrt{m}$.

Table 2. Summary of 5 Crack Stability Calculations

Crack Height (cm) in Shale	K_I(MPa$\sqrt{m}$)	Load Factor, F
0.5	0.63	1.065
2.0	1.16	1.003
7.0	1.26	<1
12.0	1.54	<1
62.0	2.47	<1

The calculations showed that a crack as short as 2 cm is incipiently unstable if the 7.6 MPa fluid pressure can get to it. In fact, the shortest crack is also potentially unstable if the horizontal in-situ stresses were slightly less than the assumed value of 6 MPa, or if the fluid pressure were slightly in excess of 7.6 MPa. Additionally, it is well established that K_{IC} decreases with very short crack length so that we may be over estimating the load factor, F, for the shorter cracks. Thus, the pressurizing of a small flaw in the roof shale is proposed as the most likely explanation for the observed hydrofrac vertical propagation.

2.4.3 Fracture and flow in a jointed rock mass

The following example was constructed to illustrate fracture and fluid flow in jointed rocks. Figure 10 shows a joint system (heavy lines) around a borehole, and the ends of the two discontinuous joints above the borehole which are considered as points of possible crack extension. The sequence in Figure 10 illustrates successive steps in the analysis. In this example, the fluid flows into a preexisting joint system; in other cases, the induced crack may cross the first interface. This numerical calculation also showed, for the first time, a phenomenon that had been predicted only analytically: the advancing crack front tended to open the natural fracture by inducing tensile stresses ahead of itself. In Figure 10c the crack has proceeded from the borehole and intersected a joint. The flow can now go out into the joint network. For this particular problem the flow is apportioned as shown in Figure 11. Notice how some flow occurs in almost every joint. Such fluid intrusion can promote joint slippage in two ways: by increasing fluid pressure and decreasing the stabilizing normal stress across the joint, and/or by wetting joint filling materials, thus reducing their frictional resistance. If slippage occurs on the joints, then some seismic noise can be generated, as in the following case history.

Sandia National Laboratories, Albuquerque, conducted the Multi-Well Experiment in the Western gas sand formations near Rifle, Colorado, at a depth of several thousand feet [22]. Three proximate wells were drilled, and one was hydraulically fractured. The progress of a hydrofracture in one well was monitored from a second well by passive seismic means [23]. As shown in Figure 12, Sandia found that the seismic noises originated from a zone between 6 and 24 m wide, considerably greater than the original fracture width (about 2.5 cm). FEFFLAP can demonstrate (see Fig. 11) how a large volume of rock may react to a single hydrofracture injection. This can help understand the above observations at the Multiwell site.

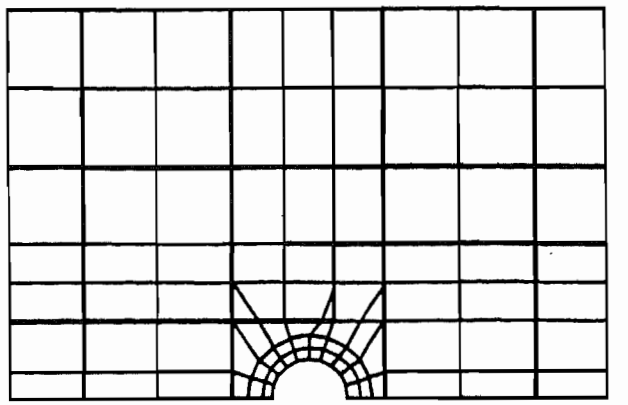

a) Pressurized hole in jointed rock

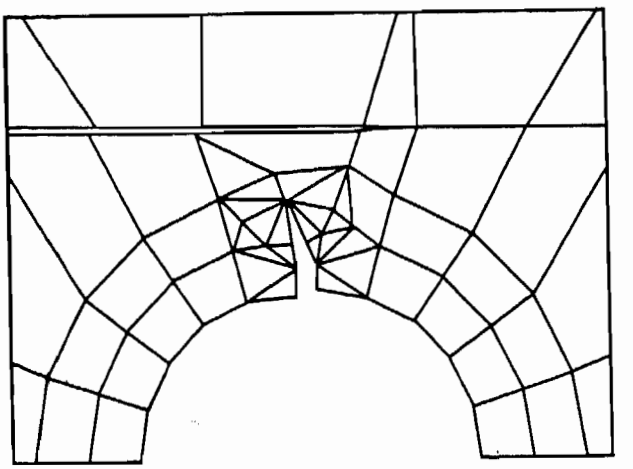

b) Fluid-driven fracture initiates from hole.

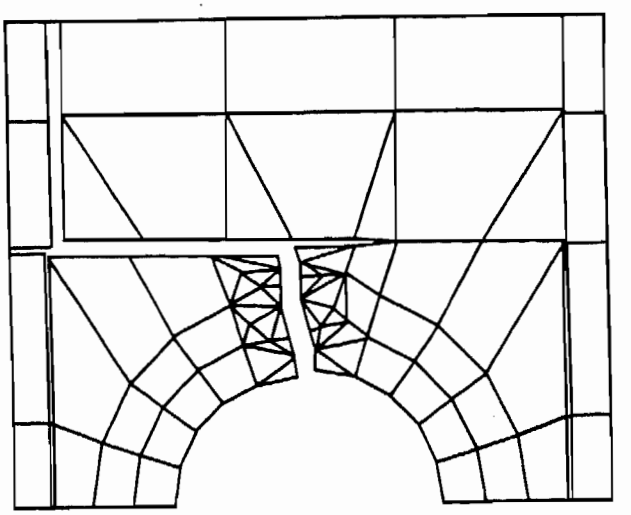

c) Fracture intersects natural joint.

Figure 10: FEFFLAP 1.0 Analysis of Fracture and Flow in a Jointed Rock Mass.

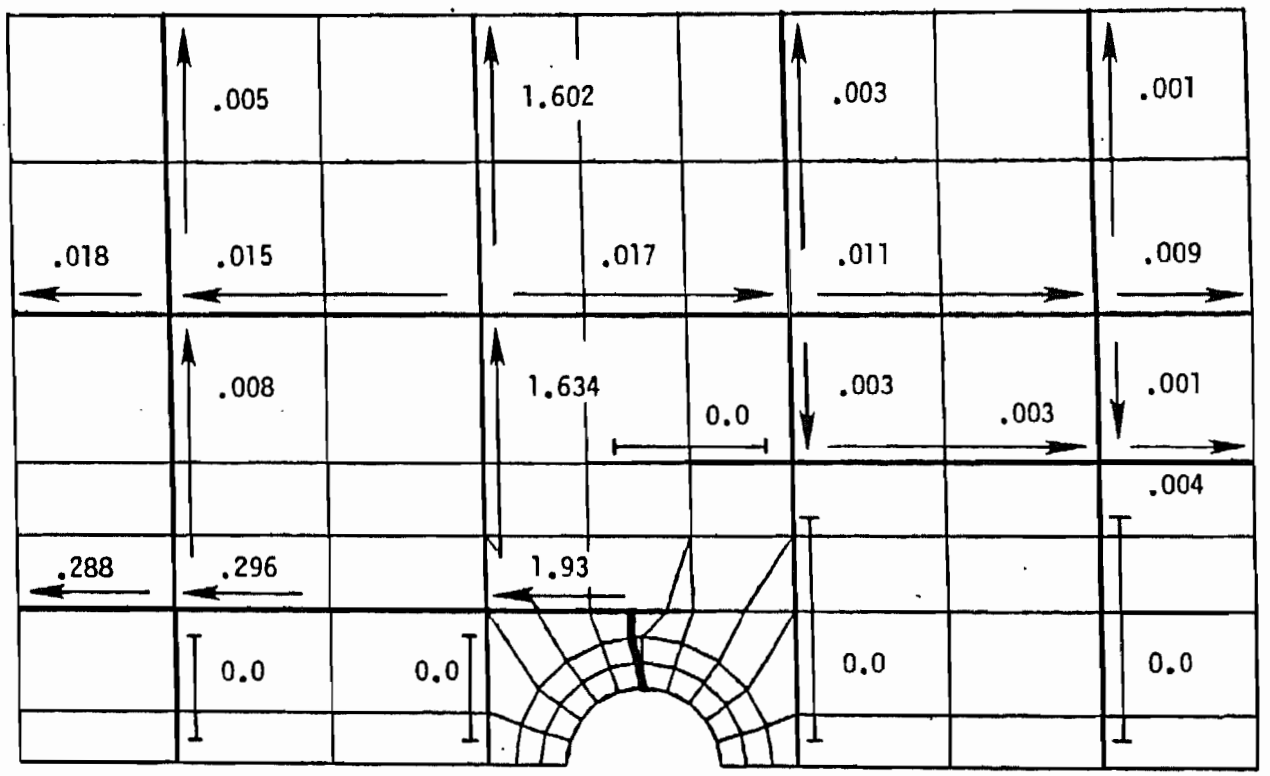

Figure 11: Apportioning of the Flow from the Steady-State Analysis of Fig. 10.

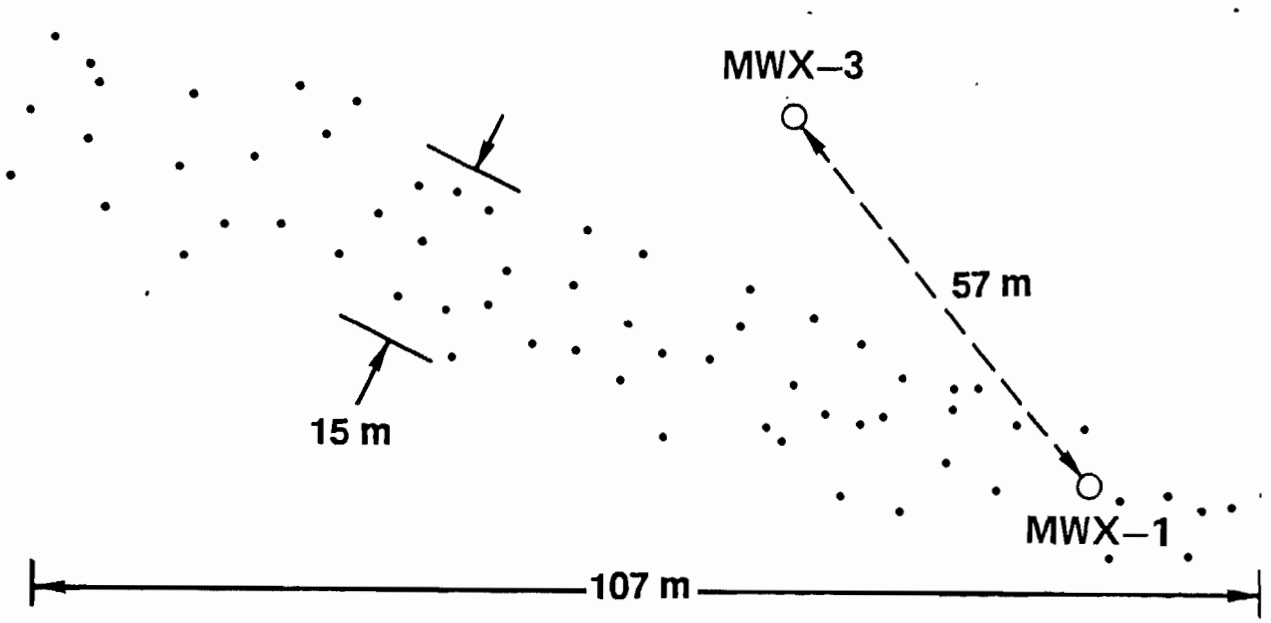

Figure 12. Microseismic Activity Due to Hydrofracturing at MWX Well No. 2, as Monitored from Well 3 [23].

3. THE TIME-DEPENDENT MODEL

3.1 Rationale for the New Developments

The value of the steady-state model development was two-fold: to establish the procedure for coupling solid/fracture mechanics and fluid flow analyses, and to provide some interesting insights in the interplay between induced fractures and natural fractures. However, this did not meet a crucial need for providing diagnostics during the execution of fracturing underground. That is, it would be very valuable to be able to tell from time-pressure records in the field what kind of interaction a fluid-driven fracture is experiencing with the rock mass. Is the fracture stopped for a time? Is it branching-out laterally? Is it restarting after an offset at an interface? These questions are particularly relevant when attempting to stimulate sandstone lenses away from wells, or attempting to contain a hydrofracture within a given horizon.

Thus, we pursued the time-dependent developments of our analyses with the expectation of providing a measure of forward modeling capability which would show features of time-pressure records corresponding to induced/natural fracture interactions. The only new element in the new model, albeit a major one, is the substitution of a transient fluid dynamics capability for the previous steady-state flow model. The new flow model is represented by the FAST (Fracturing and Simultaneous Transport) program [24] which is now part of our FEFFLAP version 2.0 model.

3.2 The FAST Fluid Dynamics Model

The FAST formulation we adopted is that developed for wedge-shaped fractures of constant height, i.e., the Geerstma-deKlerk type [25], where the fluid flow along the fracture can be described by a one-dimensional analysis in which the fluid pressure, temperature, and velocity depend upon a single independent variable, i.e., the position along the crack length.

3.2.1 Governing equations

The solid and fracture part of FEFFLAP provide the fracture width and stress intensity factors. Then, the relevant FAST equations are:

- for conservation of mass and momentum

$$\frac{\partial}{\partial t}(\rho w) + \frac{\partial}{\partial x}(\rho w u) + 2\,\rho v = 0 \tag{1}$$

$$-\frac{\partial P}{\partial x} = \frac{1}{2}\psi\frac{\rho u^2}{w} \tag{2}$$

in which ρ, u, and w are density, longitudinal velocity, and aperture, each averaged over the cross section, v is the local seepage velocity into the walls of the fracture, and ψ is the friction factor.

- for friction:

$$\psi = \psi \text{ laminar} + \psi \text{ turbulent} \tag{3}$$

$$\psi = \frac{24}{R_e} + a\left(\frac{\varepsilon}{w}\right)^b \tag{4}$$

where R_e, Reynold's number $= \dfrac{\rho u w}{\mu}$ (5)

μ is the fluid's dynamic viscosity

ε is the fracture wall roughness

a and b are coefficients

- from the above, one obtains a quadratic equation which can be solved for the velocity u:

$$\left[\frac{a}{2}\left(\frac{\varepsilon}{w}\right)^b \frac{\rho}{w}\right] u^2 + \frac{12\mu}{w^2} u + \frac{\partial P}{\partial x} = 0 \tag{6}$$

- for lateral seepage into walls containing fluid, a Darcy flow approach will give seepage velocity v as:

$$v = \frac{(P - P_\infty)}{(t-\tau)^{1/2}}\left[\frac{\beta k \varphi}{\pi \mu}\right]^{1/2} \tag{7}$$

where β is the fluid compressibility
k is the permeability
ϕ is the medium's porosity

or one can also use the so-called Carter formula

$$v = \frac{C}{(t - \tau)^{1/2}} \tag{8}$$

in which C is the so-called Carter coefficient [26].

- for fluid seepage into previously dry (or gas-filled) walls, Darcy's approach results in [27]

$$v = \left[\frac{k\Delta P}{2\mu t}\right]^{1/2} \tag{9}$$

where ΔP is the pressure gradient across the penetration depth into the previously unwetted medium.

3.2.2 Numerical solution procedure

The details of the solution procedure are found in [24]. In brief, the numerical solution procedure is an approximate one. At each successive time step, a pressure profile is selected from a family of curves based on four parameters:

- the pressure at the inlet
- the pressure at the leading edge
- the penetration depth of the flow
- a quantity m, which is a measure of the pressure profile's curvature.

The parameters are chosen such that the continuity equation is satisfied in a global or "integral" sense over two or three regions of the flow, including: (1) the entire volume of the fracture, (2) a small subvolume at the leading edge of the flow, and sometimes (3) the borehole or cavity volume which feeds the fracture. The other equations (including momentum, and energy) are all satisfied on a local basis which is "exact" within the tolerances of numerical quadrature routines. As a numerical convenience, the pressure profile and all other dependent variables are represented by their values at discrete grid points, along the fracture; a few points (ca.6) are usually sufficient. Experience has shown that fracture speed and length are not sensitive to the chosen family of profiles.

3.3 The Coupling of FAST to FEFFLAP

We begin a time step with the crack tip(s) located at fixed point(s) on the grid, as determined from FEFFLAP's solid/fracture analysis. FAST is then called on to generate a provisional solution, including the pressure profile along the crack and the propagation speed. FEFFLAP, in turn, is called to generate new values of crack width (w) and stress intensity factor (K_I) corresponding to the new pressure profile. The next call to FAST uses the new values of w, K, and pressure to generate a better candidate for the pressure profile, and so on. The progress of iterations is judged by monitoring the convergence of the pressure profile and stress intensity.

Note that FAST only uses the Mode I stress intensity factor to adjust the pressure profile, because the FAST model is that of a crack propagating in-plane. However, FEFFLAP does not have that restriction, and can propagate cracks in mixed-mode. At the end of a FAST cycle a new crack direction can be determined by FEFFLAP, if warranted. Thus the effect of the FAST limitation is only to restrict crack propagation to linear increments. The overall fracture, however, can curve as guided by the stress field and material properties.

To model the interaction among multiple fractures we have developed a procedure which allows FAST to process one crack at a time, thereby obtaining a new pressure profile for each crack, individually. Once pressure boundary conditions have been determined for all the cracks, FEFFLAP calculates the displacements along all the cracks, simultaneously, such that any one crack can influence all the others. The algorithms are written in a fashion which allows the user to monitor the progress of the calculations and interactively tailor the iteration sequence to obtain better convergence.

When the FAST/FEFFLAP iterations have reached the desired degree of convergence, the problem is advanced by a time increment Δt. Tip speeds, $\dot{L}$, are available for all the cracks and FEFFLAP has determined the direction of propagation for each. So each of the cracks can be shifted forward by $\Delta L = \dot{L}\,\Delta t$, in the direction appropriate for mixed mode fracture, if necessary.

3.4 Verification and Validation of FEFFLAP 2.0/FAST

3.4.1 Analytical solution for gas-driven fractures with constant borehole pressure

Figure 13 shows a geometry of interest for gas-driven fracturing from a borehole, where 2 fractures have begun to dominate. A FEFFLAP analysis was performed of that geometry with the following conditions:

borehole radius	0.1 m	Poisson's ratio	0.3
borehole pressure	40 MPa	surface roughness	400 μm
borehole temperature	300°KV	rock porosity	0.3
confining stress	10 MPa	gas viscosity	10^{-5} Pa-S
fracture toughness	0	molecular weight	28
shear modulus	3 GPa	ambient pore pressure	0.1 MPa

The rock permeability was assumed negligible in order to permit comparison with an analytical, self-similar solution for the extension of the major cracks [28]. Noting that the similarity solution requires cracks to be long with regard to borehole diameter, Figure 14 shows a very good agreement between the FEFFLAP computation of crack speed gradient and the analytical solution at crack length exceeding 5 borehole diameters.

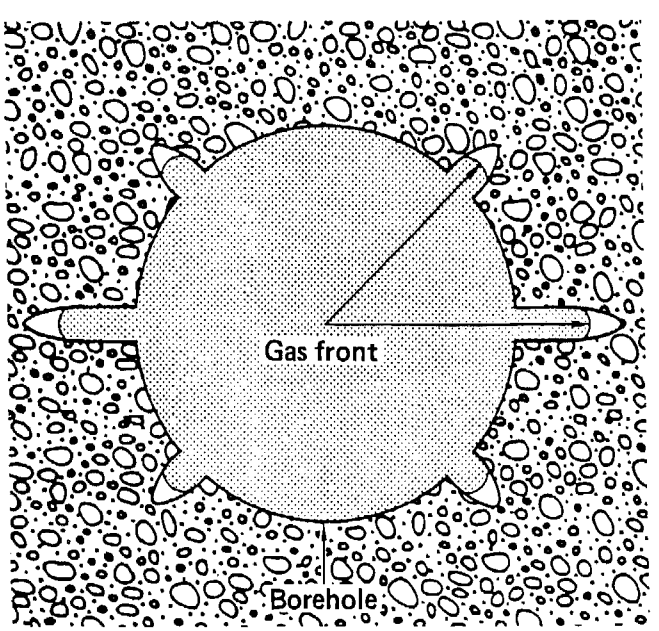

Figure 13. Geometry for FEFFLAP/FAST Analysis of Multiple Gas-Driven Fractures.

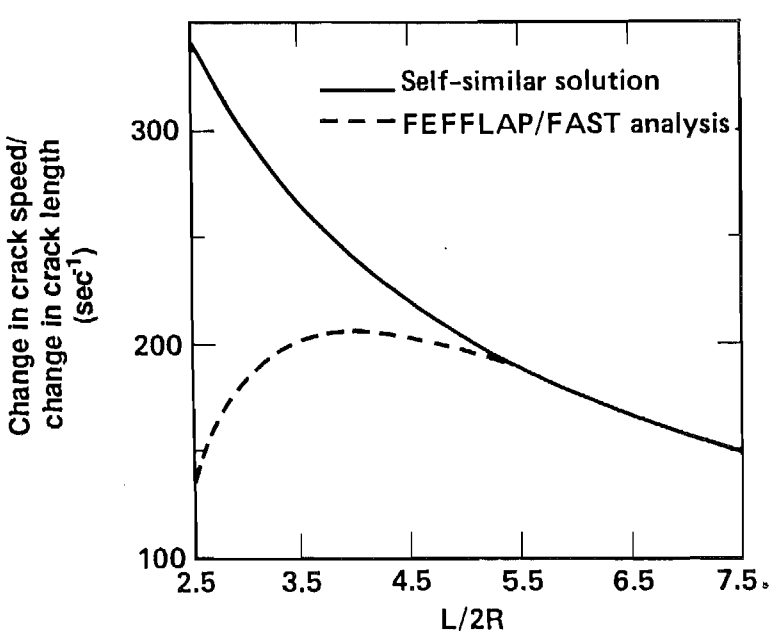

Figure 14. Comparison of FEFFLAP Results With Those of a Similarity Solution [28].

3.4.2 Analytical solutions for laminar incompressible fluid flow, with constant flow rate.

Geerstma and deKlerk analytically obtained approximate solutions for a two-wing wedge-shaped fracture driven by the laminar flow of an incompressible fluid injected at constant flow rate [25]. At early times, seepage losses are negligible and the fracture grows as

$$L = 0.48 \left[\frac{G\,Q^3}{(1-\nu)\mu}\right]^{1/6} t^{2/3} \tag{10}$$

where G is the elastic shear modulus of the medium.

At late times, seepage losses change the growth to

$$L = \frac{1}{2\pi}\,\frac{Q}{C}\,t^{1/2} \tag{11}$$

where C is the Carter seepage loss coefficient.

Recasting in terms of crack velocity:

$$\dot{L} = \frac{2}{3}\left[0.48\left[\frac{G\,Q^3}{(1-\nu)\mu}\right]^{1/6}\right]^{3/2}\left[\frac{1}{L}\right]^{1/2} \quad \text{(early)} \tag{12}$$

$$\dot{L} = \frac{1}{2}\left[\frac{Q}{2\pi C}\right]^2 \frac{1}{L} \quad \text{(late)} \tag{13}$$

Results of FAST calculations in stand-alone and FEFFLAP 2.0/FAST with the mesh of Figure 15, are compared to the above analytical results in Figure 16. The agreement is excellent over a wide range of fracture speed and fracture length. This is true even though the FEFFLAP code does not include the inertial effects of the solids; however, the maximum calculated crack speeds were no more than about 100 m/s, which is a small fraction of the shear wave speed. Other models could be used to estimate how important these effects become at much higher crack speeds [29,30].

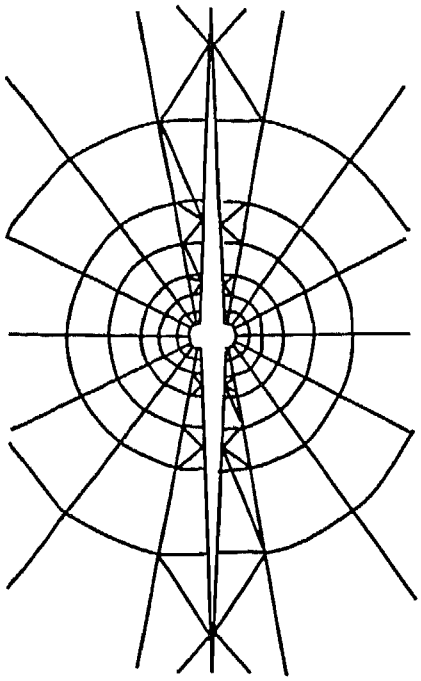

Figure 15. Mesh for FEFFLAP 2.0 Calculation. Constant Flow Rate.

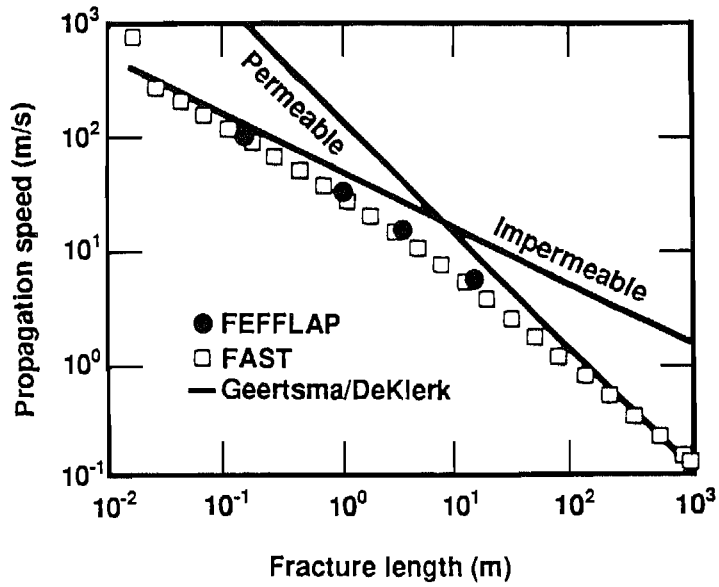

Figure 16. FEFFLAP 2.0 Results Compared to FAST, and to Analytical Results from [25].

3.4.3 Validation against physical block tests.

Recently, much more sophisticated block tests than the ones described in 2.3 were performed at LLNL to provide physical benchmarks against which to validate our numerical developments. Details are contained in the companion paper and in references [31,32].

In summary, three block tests (A,B,C) were performed. They involved sandstone tablets (lenses) embedded in gypsum cement (Figure 17). These experiments revealed the progression of fluid-driven fractures through the sandstone lenses. The fractures were forced to initiate and propagate from a high pressure steel tube that was slotted on one side. Also, a wrap-around tape, extending out about 2 cm, kept the cement from entering the steel tube while pouring, and directed the crack into a sympathetic stress field. The fractures were constrained to travel unilaterally and the fracture front was determined by resistance changes denoting the rupture of thin tungsten wires embedded perpendicular to the fracture plane. To maintain constant height, the fracture was contained in the vertical direction by wire mesh screens embedded near the top and bottom of the block, and perpendicular to the injection tube. The screens and sandstone tablet were anchored using piano wire

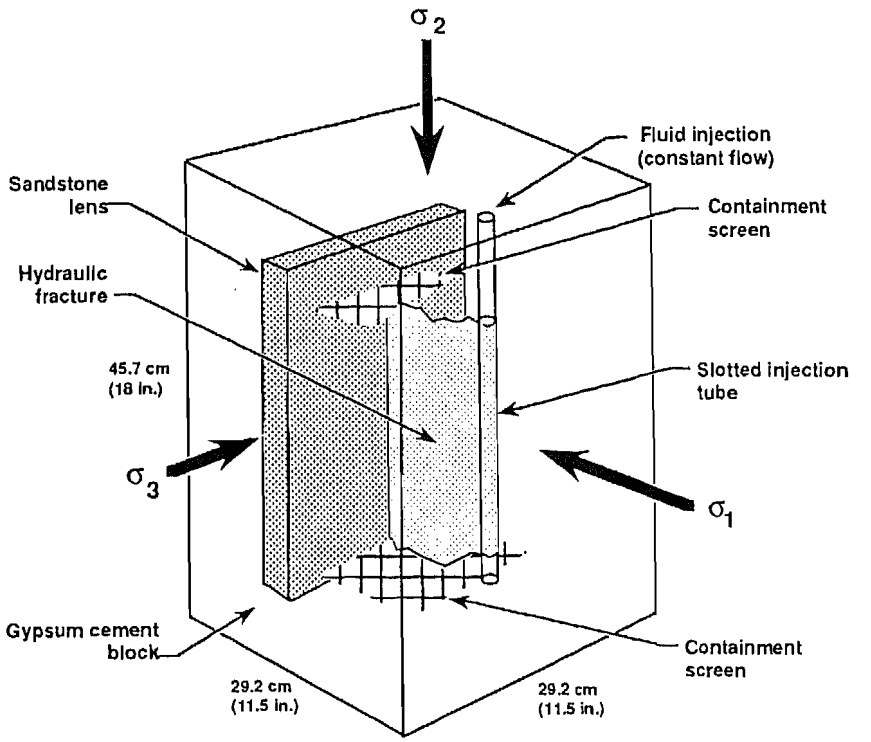

Figure 17. Schematic of Block-Fracturing Experiments.

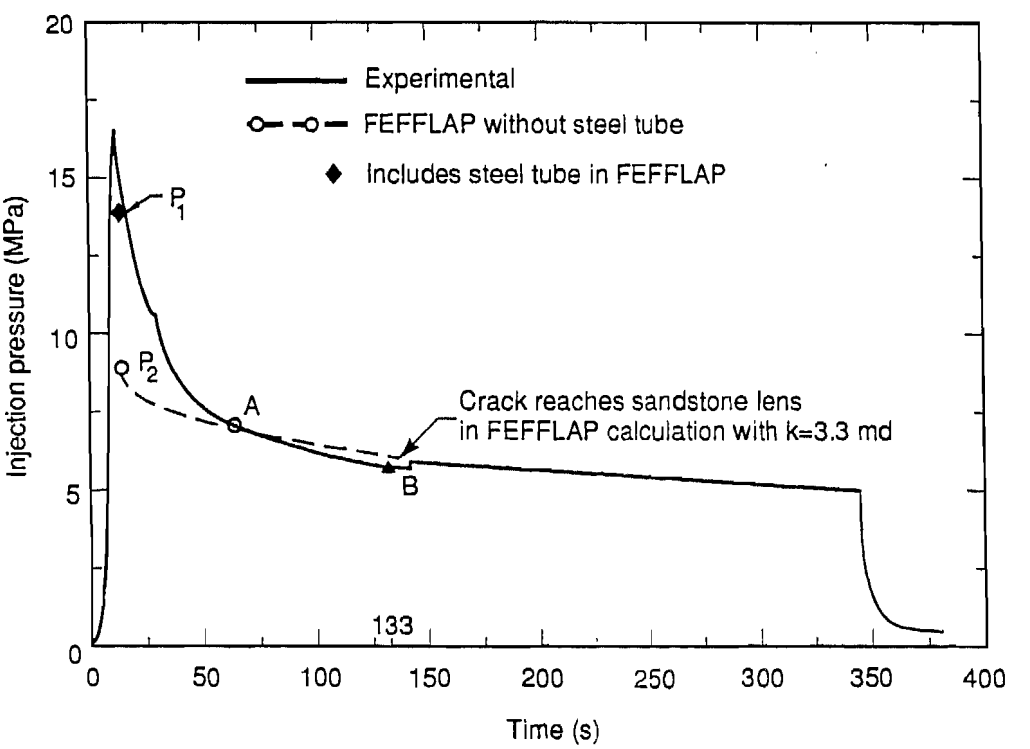

Figure 18. Pressure-time record for test B, vs. FEFFLAP pressure-time history.

stretched across the mold, and the gypsum cement was prepared carefully, according to pre-planned procedures of sifting, wetting, mixing, and pouring. A light oil was used to propagate the fracture and was pumped at a steady rate with a ball-screw piston. The blocks were triaxially loaded for the duration of crack propagation. The injection pressure was closely monitored during the fracturing process. Figure 18, corresponding to test B, is given as an example to provide data for comparison with calculations. Crack velocity was estimated from the breakage times of the embedded wires (points A and B on Figure 18). After fracturing, the blocks were dissected to show the exact fracture outline, as well as the extent of leakoff. Dissection of the blocks showed them to be very homogeneous.

A cross-section representing the gypsum block geometry was meshed for analysis with FEFFLAP and is shown in Figure 19. First, two calculations were performed without modeling the steel injection tube. The cracks were advanced to the times when they just reached the sandstone lens. Crack length at this point was 12.7 cm. Propagation was not continued through the lens in the calculation because the sandstone is more permeable and, in the experiment, we believe that the crack essentially stopped while fluid filled the lens and then the crack restarted. FEFFLAP has no flow storage capability, at present, to model such a phenomenon. A pressure-time curve was generated from the successive crack tip locations during propagation. The curve is superimposed on the experiment record on Figure 18, for comparison purpose. Early pressures are not expected to compare well because of the steel tube and of the tape used to start and direct the fracture initially. In fact, the tip location next to the borehole where the crack initiates is not included in the curve because a pressure was not calculated due to coarseness of the finite element mesh there. Later pressures compare well with the experimental results.

The pressure profile down the crack, and the crack shape from the numerical results at 11.5 cm (largest crack length before interface is intersected) are shown on Figures 20 and 21, respectively; results are given for both permeabilities, k = 3.3 and 15 millidarcy. When the crack reached 11.5 cm, the fluid front had just reached the tip of the propagating crack at the highest leakoff rate and was already there at the lower leakoff rate. However, at early times (not shown) the fluid did not reach the crack tip for either permeability. The pressure profile is slightly higher near the borehole for greater leakoff. For either value of k, pressure falls off rather quickly

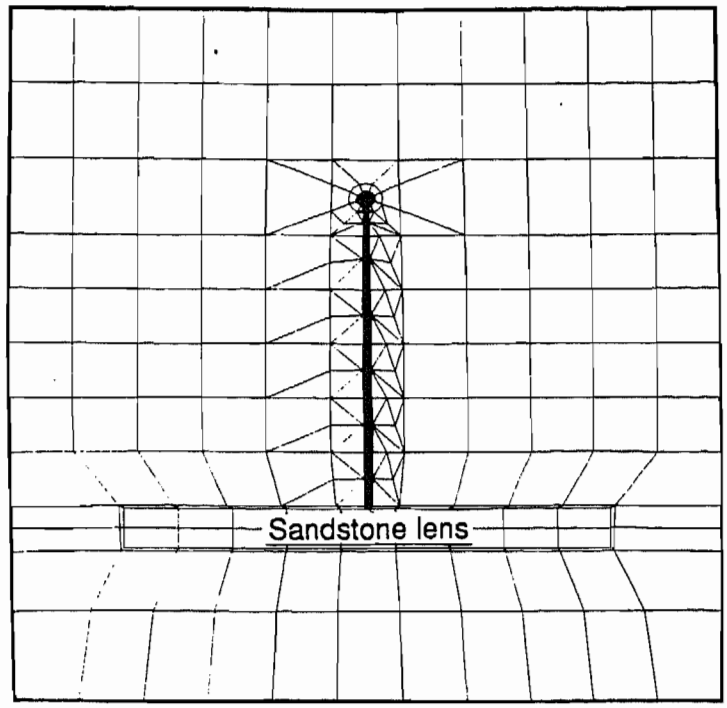

Figure 19. Finite Element Mesh for FEFFLAP 2.0 Analysis of Crack Propagating from Borehole to Sandstone Lens in Gypsum Block.

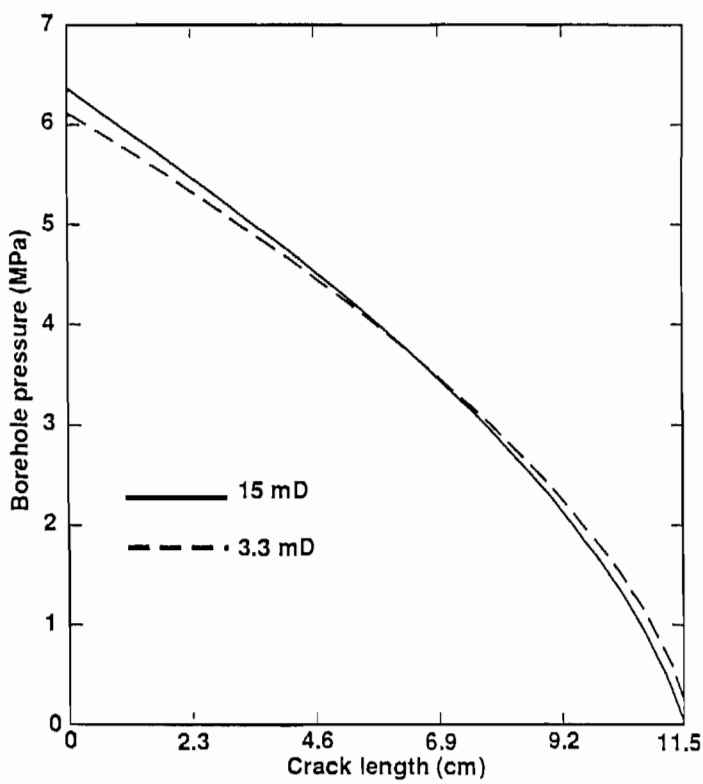

Figure 20. Pressure Profiles as Crack Nears Lens, for Two Values of Permeability.

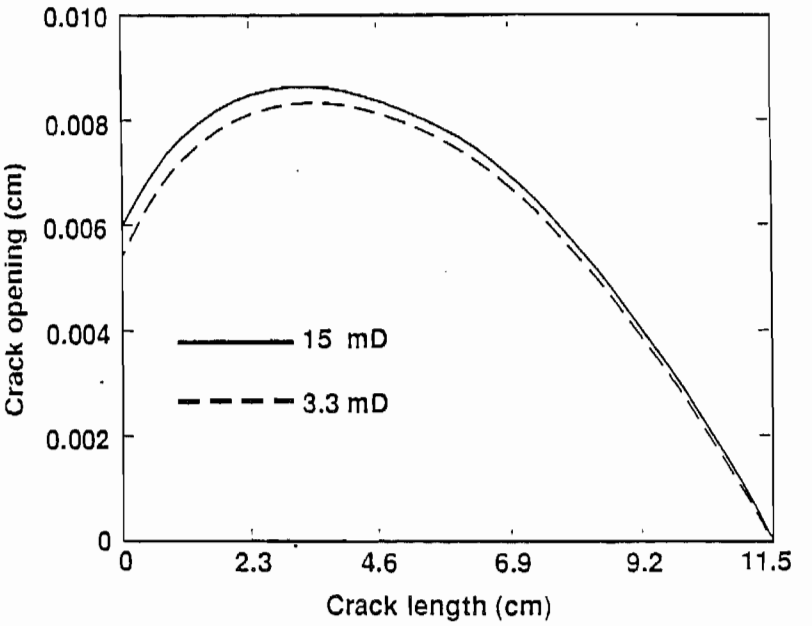

Figure 21. Crack Shape as Crack Nears Lens, for Two Values of Permeability.

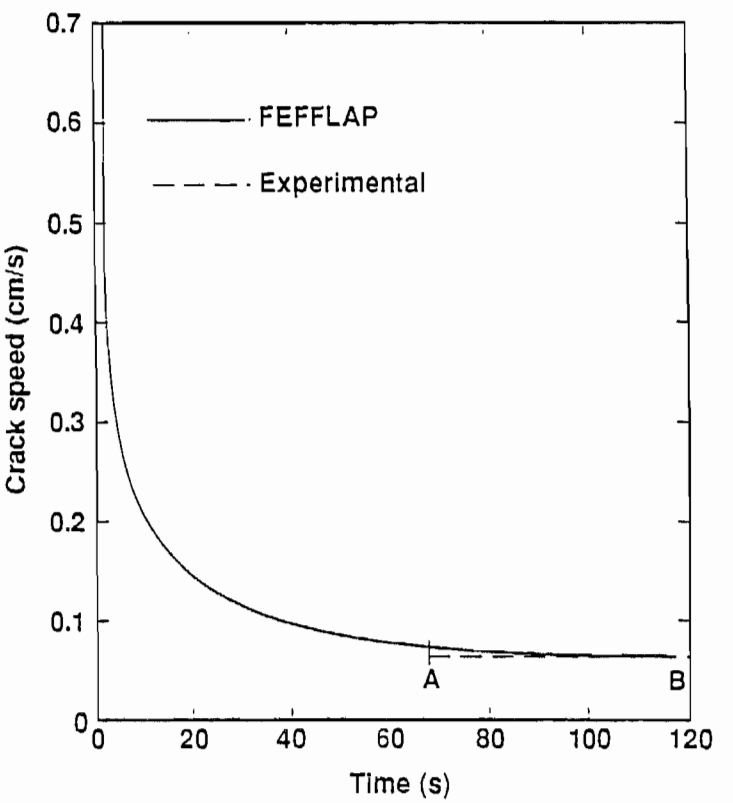

Figure 22. Decay of Crack Tip Velocity as Crack Extends (k=3.3 md). The experimental Value Corresponds to an Average Value Computed Between Points A and B on Figure 18.

due to leakoff. Notice the ballooning of the crack, a feature of a single-wing crack in which the borehole constrains one end of the crack. This ballooning is not much influenced by the value of k. Figure 22 shows the calculated crack tip velocity as a function of crack length for k = 3.3 millidarcys. Crack velocity decreases quickly as the crack extends and then decreases slowly. At later times, the crack velocity agrees very well with the experimental value determined from points A and B on Figure 18 (where the wires broke). We noted that for k = 15 md the late-time crack tip velocity was slowed by a factor of 44, but fluid velocity at the inlet was slowed by only 3%. Another calculation with k = 3.3 md was performed, that included the elastic effects of the steel tube in the borehole. In this case, the early crack extension required a higher pressure, as shown by Point P_1 on Figure 18, due to the higher stiffness of the tube. The pressure is in reasonable agreement with the experimental value. At late times the effects of the tube should be minimal.

The above results can be considered a measure of validation of FEFFLAP 2.0.

3.5 Examples of Application

To illustrate the capabilities of the time-dependent model, FEFFLAP 2.0 was set up to simulate gas-driven development of multiple fractures around boreholes, as can be performed to stimulate gas-well production with solid propellants.

First, a symmetric problem was run with multiple cracks; for this case, six cracks were made to emanate from a borehole at 60° intervals (Figure 23). This geometry was chosen because each crack is identical to every other crack. Cracks can be extended in the model by either specifying a length or a time of propagation (the model then returns the corresponding time or length). In this test case, the cracks were extended by specifying an equal length for each. Once the crack length is specified, all the other values are calculated in the FEFFLAP model. If the FEFFLAP model is working correctly, it will return the same parametric values for all the cracks. These parametric values are given in Table 3 for the upper three cracks in Figure 23. From symmetry, the values for the lower three cracks are identical to those for the upper three cracks. The aperture represents the crack opening at the borehole. All parameters agree well. Since the cracks have the same speed, they will extend together and continue being of equal length.

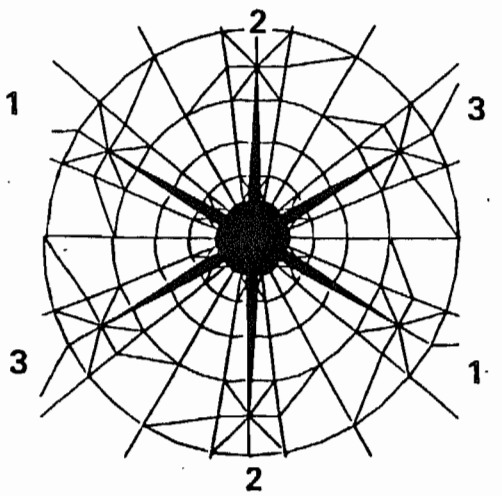

Figure 23. Six-fold Symmetric Cracking from a Borehole. All Cracks Propagate Radially Outward at the Same Speed.

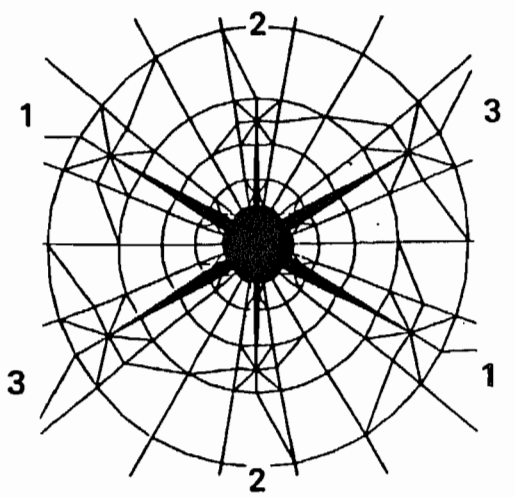

Figure 24. Two-fold Symmetric Cracking from a Borehole. The Long Cracks are Extending Nearly Three Times Faster Than the Short Cracks.

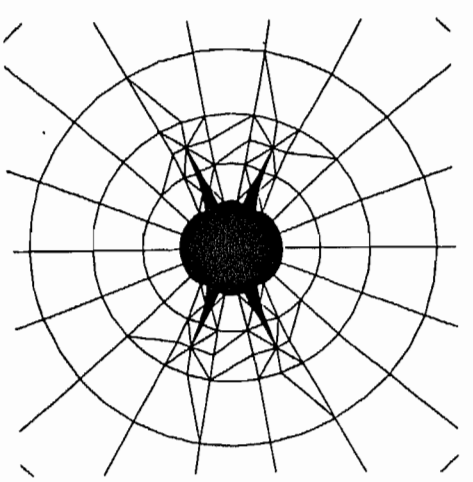

Figure 25. Cracking from a Borehole, in which Propagating Cracks Repel Each Other.

Table 3. Parametric Values for 6-Fold Symmetric Crack Problem.

Crack Number	Time (sec)	Length (m)	Speed (m/sec)	Aperture (m)
1	.003324	.403	177.5	.00189
2	.003300	.400	176.4	.00188
3	.004416	.402	178.9	.00190

After this first check had been performed on the model, less symmetric problems were addressed. The first choice was to make a small change in the previous configuration, by making one of the cracks shorter. For this problem the cracks were propagated again in their own plane. The FEFFLAP solution is shown in Figure 24. The smaller aperture of the shorter crack is clearly seen. Parametric values for this case are given in Table 4. It is interesting to note that although the short cracks are 60% of the length of the longer cracks, their speed is about 1/3 of that of the longer cracks. This means that the shorter cracks will die out quickly in favor of the longer cracks.

Table 4. Parametric Values for 2-Fold Symmetric Crack Problem.

Crack Number	Time (sec)	Length (m)	Speed (m/sec)	Aperture (m)
1	.003422	.407	232.4	.00222
2	.002005	.243	84.6	.00085
3	.003408	.405	232.9	.00221

Figure 25 illustrates what happens when even less symmetric cracking takes place. The cracks that are close to each other tend to repel each other. To our knowledge this result has not been obtained before. In this example crack tip speed was about 10% of shear-wave speed.

4. SUMMARY - DISCUSSION

4.1 Summary

We have pursued a joint numerical and experimental program designed to gain insight in the interaction of induced fluid-driven fractures with natural discontinuities in rock masses.

The numerical developments resulted from the coupling of several building blocks: (1) a solid and fracture mechanics model capable of representing mixed-mode fracture propagation in arbitrary stress fields, (2) models of rock discontinuities which account for nonlinear joint behavior, and (3) models of fluid flow for both liquids and gases, covering the steady-state as well as the transient time-domain. The steady-state coupled model is the 2-dimensional finite element program FEFFLAP 1.0, and the transient model is the FEFFLAP 2.0 version with the FAST fluid dynamics algorithm. Both these models have been verified against analytical solutions for fluid-driven cracks.

In addition, a measure of validation of these numerical models was achieved by comparison with the results of physical experiments. These consisted of blocks of different rock simulants, with interfaces and/or inclusions, which were hydraulically fractured. The calculated fracture paths and pressure-time histories compared well to results obtained with the physical model.

4.2 Discussion

Whereas there is a plethora of hydrofracture simulation models based on continuum assumptions, we believe that the above developments are so far unique in tackling fluid-driven fracturing in discontinuous media.

On the other hand, we are well aware of the limitations of our work, which are yet to be removed:

- the FEFFLAP formulation is applicable to fractures of constant height (the Geertsma-deKlerk type); this does not account for 3-dimensional aspects of hydrofracturing or gas fracturing.

- the inertial behavior of the fluids is accounted for, but not that of the solids. This is acceptable as long as fracture speed is only a small fraction (say less than 10%) of the maximum fracture speed, which is considered to be the shear wave speed in the medium. But simulations at higher fracture speeds could require that the solid dynamics also be included.

- the model does not account for storage of fluids in the adjacent medium in a rigorous fashion. This, for example, has limited our modeling of a driven crack transecting an embedded permeable lens.

- finally, the transient intersection of driven cracks, with natural fractures remains to be validated, including correct apportioning of the flow between several cracks evolving dynamically from an intersection.

Clearly, the field of simulation of fluid-fracturing in real rock masses continues to be rich in opportunities for future developments.

5. REFERENCES

1. Veatch, R. W. (1983) "Overview of Current Hydraulic Fracturing Design and Treatment Technology - Part 1, J. Petroleum Technology, pp 677-687, April.

2. Veatch, R. W. (1983) "Overview of Current Hydraulic Fracturing Design and Treatment Technology - Part 2, J. Petroleum Technology, pp 853-864, May.

3. Mendelsohn, D. A. (1984) "A Review of Hydraulic Fracture Modeling - Part 1: General Concepts, 2D Models, Motivation for 3D Modeling", ASME J. Energy Resources Technology, v. 106, pp 369-376, Sept.

4. Mendelsohn, D. A. (1984) "A Review of Hydraulic Fracture Modeling - Part 2: 3D Modeling and Vertical Growth in Layered Rock", ASME J. Energy Resources Technology, v. 106, pp 543-553, Dec.

5. Cleary, M. P. (1988) "The Engineering of Hydraulic Fractures. State of the Art, and Technology of the Future", J. Petroleum Technology, pp 13-21, Jan.

6. Boone, T. J., Ingraffea, A. R., and Roegiers, J. C. (1989) "Visualization of Hydraulically-Driven Fracture Propagation in Poroelastic Media Using a Superworkstation", J. Petroleum Technology, pp 574-580, June.

7. National Research Council, (1983) "Hydraulic Fracturing Stress Measurements", Proceedings of a Workshop, 270 p., (National Academy Press, Washington, D.C.), 270 p.

8. Weeren, H. O., Coobs, J. H., Haase, C. S., Sun, R. J., and Tamura, T. (1982) "Disposal of Radioactive Wastes by Hydraulic Fracturing", Oak Ridge National Laboratory, Oak Ridge, TN, Report ORNL/CF-81/245, 144 p., May.

9. Warpinski, N. R. (1985) "In-Situ Measurements of Hydraulic Fracture Behavior. PTE-3 Final Report", Sandia National Laboratories, Report SAND 83-1826, 172 p., July.

10. Heuze, F. E. (1986) "The Unconventional Gas Program at the Lawrence Livermore National Laboratory", UCID-20610, 25 p., Jan.

11. Heuze, F. E. (1987) "Status of the Western Gas Sands Project at Lawrence Livermore National Laboratory", Lawrence Livermore National Laboratory, UCID-21108, 13 p., July.

12. Ingraffea, A. R., Gerstle, W., Gergely, P., and Saouma, V. (1984) "Fracture Mechanics of Bond in Reinforced Concrete", ASCE J. Struct. Div., v. 110, n. 4, pp 871-890.

13. Heuze, F. E. (1981) "JPLAXD: A Finite Element Program for Static, Plane and Axisymmetric Analysis of Structures in Jointed Rock", Lawrence Livermore National Laboratory, UCID-19047, 50 p., May.

14. Noorishad, J., Witherspoon, P. A., and Brekke, T. L. (1971) "A Method for Coupled Stress and Flow Analysis of Fractured Rock Masses", Geotechnical Eng. Publ. No. 71-6, University of California, Berkeley, March.

15. Ingraffea, A. R., Shaffer, R. J., and Heuze, F. E. (1985) "FEFFLAP: A Finite Element Program for Analysis of Fluid-Driven Fracture Propagation in Jointed Rock, Vol. 1: Theory and Programmer's Manual", Lawrence Livermore National Laboratory, UCID-20368, 64 p., March.

16. Shaffer, R. J., Ingraffea, A. R., and Heuze, F. E. (1985) "FEFFLAP" A Finite Element Program for Analysis of Fluid-Driven Fracture Propagation in Jointed Rock, Vol. 2: User's Manual and Model Verification", Lawrence Livermore National Laboratory, UCID-20369, 74 p., March.

17. Sih, G. C. (1973) Handbook of Stress Intensity Factors, (Institute of Fracture and Solid Mechanics, Lehigh Univ., Bethlehem, PA).

18. Ouchterlony, F. (1982) "Analysis of Cracks Related to Rock Fragmentation", Part 1 of Lectures at the International Center for Mechanical Sciences (CISM), Udine, Italy, Report DS 1982:4.

19. Thorpe, R. K., Heuze, F. E., and Shaffer, R. J. (1984) "An Experimental Study of Hydraulic Fracture-Interface Interaction", Lawrence Livermore National Laboratory, Livermore, CA, UCID-20114, 39 p. July.

20. Shaffer, R. J., Thorpe, R. K., Ingraffea, A. R., and Heuze, F. E. (1984) "Numerical and Physical Studies of Fluid-Driven Fracture Propagation in Jointed Rock", Proc. 25th U.S. Symp. on Rock Mechanics, Evanston, IL, pp 117-126 (Soc. Mining Eng., Littleton, CO).

21. St. John, C. M. (1971) "Three-Dimensional Analysis of Rock Slopes", in Proc. Symp. Int. Soc. Rock Mech., Nancy, France, Sept.

22. Finley, S. J. Ed. (1988) "Final Technical Poster Session for the Multiwell Experiment, SPE/DOE Symposium on Low Permeability Reservoirs", Sandia National Laboratories, Albuquerque, NM, SAND 88-2678, 85 p., Nov.

23. Thorne, B. J., and Morris, H. E. (1988) "Passive Seismic Monitoring of Hydraulic Fracture Experiment at the Multiwell Experiment Site", Sandia National Laboratories, Albuquerque, NM, SAND 88-1284, 61 p., August.

24. Nilson, R. H., and Peterka, D. L. (1986) "User's Manual for the FAST Hydrofracture Code", Report to Lawrence Livermore National Laboratory, by S-CUBED, La Jolla, CA, UCRL-15852, August.

25. Geertsma, J. and F. DeKlerk (1969) "A Rapid Method for Predicting the Width and Extent of Hydraulically Induced Fractures, J. Petroleum Tech., v. 21, pp 1571-1581.

26. Howard, G. C. and Fast, C. R. (1970) "Hydraulic Fracturing", Monograph Volume 2 (Soc. Petroleum Eng., Richardson, TX).

27. Heuze, F. E., Shaffer, R. J., Blair, S. C., and Thorpe, R. K. (1989) "Understanding the Effect of Natural Fractures on the Hydrofracture Stimulation of Natural Gas Reservoirs", Lawrence Livermore National Laboratory, UCRL-100229. Also available as SPE 18956, SPE Joint Rocky Mountain Regional Meeting and Low Permeability Reservoir Symposium, Denver, CO, March.

28. Nilson, R. H. (1981) "Gas-Driven Fracture Propagation", ASME J. Applied Mechanics, v. 45, pp 757-762.

29. Swenson, D. (1985) "Modeling Mixed-Mode Dynamic Crack Propagation Using Finite Elements", Ph.D. Thesis, Dept. of Civil Engineering, Cornell Univ., Ithaca, NY, 212 p.

30. Swenson, D. V., and Ingraffea, A. R. (1987) "A Finite Element Model of Dynamic Crack Propagation with an Application to Intersecting Cracks", Proc. 4th Int. Conf. Numerical Meth. in Fract. Mech., San Antonio, TX, March 23-27, pp 191-204 (Pineridge Press, Swansea, U.K.).

31. Blair, S. C., Thorpe, R. K., and Heuze, F. E. (1988) "Physical Models of Hydrofracturing Across Material Interfaces", Lawrence Livermore National Laboratory, UCID-21505, 28 p., October.

32. Blair, S. C., Thorpe, R. K., Heuze, F. E., and Shaffer, R. J. (1989) "Laboratory Observations of the Effect of Geologic Discontinuities on Hydrofracture Propagation", Proc. 30th U.S. Symposium on Rock Mechanics, pp 443-450, Morgantown, WV (A. A. Balkema, Brookfield, VT).

6. ACKNOWLEDGMENTS

This work was performed by the Lawrence Livermore National Laboratory under contract W-7405-Eng-48 with the U. S. Department of Energy, as coordinated through the Morgantown Energy Technology Center.

We thank Lydia Grabowski for her fine typing of the manuscript.